XIV International Conference on Computational Plasticity. Fundamentals and Applications
COMPLAS 2019
E. Oñate, D.R.J. Owen, D. Peric , M. Chiumenti, and Eduardo de Souza Neto (Eds)

MODELLING OF WIDTH CONTROL FOR HOT STRIP MILL WITH FEM ANALYSIS

MASAYASU SEKIMOTO[*], MITSUHIKO SANO[†] AND KAZUHIRO OHARA[†]

[*†] Toshiba Mitsubishi-Electric Industrial Systems Corporation (TMEIC)
3-1-1 Kyobashi, Chuo-ku, Tokyo 104-0031, Japan
email: SEKIMOTO.masayasu@tmeic.co.jp, http://www.tmeic.com

Key words: FEM, Simulation, Hot Rolling, Width.

1 INTRODUCTION

In this paper, we discuss the modeling and simulation results of FEM analysis for width rolling for hot strip mill. The number of standard widths that can be produced efficiently in a continuous slab caster feeding a hot strip mill is limited. This has increased the requirement for width reduction in the hot strip mill rolling stands. The width of a slab can be reduced using vertical edger rolling stands in the roughing mill section and by using a slab sizing press. Effective width control using the vertical edgers is important for achieving the accuracy and precision of slab width relative to target values. In addition, effective width control can reduce width fluctuation caused by non-uniform deformation in head and tail part of the slab. The slab sizing press, which is designed to directly press the sides of the slab within molds, can be used to efficiently reduce width over the entire length of the slab. However, due to the physical layout and to construction constraints, the addition of a slab sizing press is not possible in many of the hot strip mills currently in operation. If the installation of a slab sizing press is not possible, the requirement for large width reduction must be accomplished entirely by using the vertical edgers. The width reduction capability of the vertical edgers is often limited since the vertical edgers are normally used only during forward passes in roughing mill. It is possible to increase the width reduction capability by modifying mill operation to use the vertical edgers on both forward and reverse passes. The modified rolling operation is referred to as VVH rolling because of the order of the rolling sequence. First step, vertical edger rolling on a reverse pass (width reduction). Second step, vertical edger rolling on a forward pass (width reduction). Final step, horizontal mill rolling (thickness reduction). However, the behavior of width deformation in VVH rolling is different from standard, forward pass only, edger rolling.

Three-dimensional width deformation of a slab when using VVH rolling was analyzed by FEM (Finite Element Method). The influence of various parameters including slab width, slab thickness, and the distribution pattern of width draft between forward and reverse passes were investigated and their impact on deformation phenomena were studied. Using the results of our analysis, we developed an optimal distribution pattern of width draft between forward and reverse passes for VVH rolling.

2 ROLLING PROCESS IN HOT STRIP MILL AND ROUGHING MILL

An example of conventional hot rolling mill configuration is shown in Figure 1. A slab is heated in the reheating furnace to around 1200 ºC then discharged onto the roughing mill passline and moved to the roughing mill stands using horizontal roller tables. The slab is rolled using several passes in the roughing mill to produce a transfer bar. Vertical edgers, located adjacent to the horizontal rolling stand(s), are used to reduce the slab width to the target value. When the slab has been rolled to the transfer bar target values for width and thickness, the transfer bar is then fed into the finishing mill where the thickness is reduced in each successive rolling stand to produce the target strip thickness. The strip is then cooled as it travels along the run out table to its target coiling temperature.

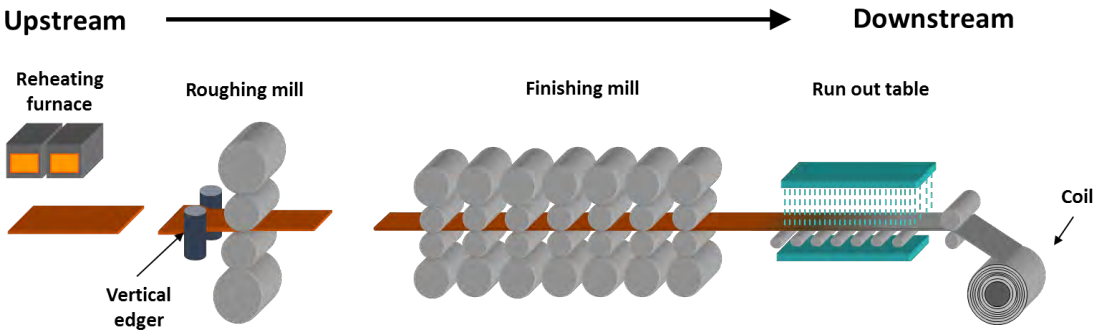

Figure 1: Overview of conventional hot rolling mill

During several passes in the roughing mill, slab width is reduced using the vertical edger and slab thickness is reduced using the horizontal mill. The typical width reduction sequence in the roughing mill is shown in Figure 2. During forward passes, slab moving in the upstream to downstream direction, the slab width is reduced using the vertical edger and thickness is reduced using the horizontal mill. During reverse passes, slab moving in the downstream to upstream direction, only slab thickness is reduced using the horizontal mill.

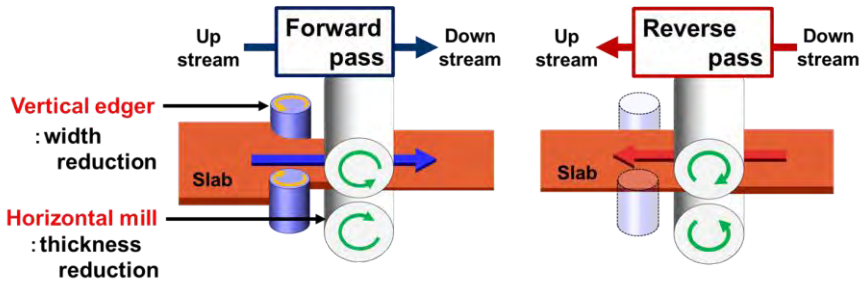

Figure 2: Standard rolling sequence in roughing mill

When using the VVH rolling sequence, slab width is reduced during both forward and reverse passes. A comparison of the standard sequence and the VVH sequence are shown in Figure 3 (Top view).

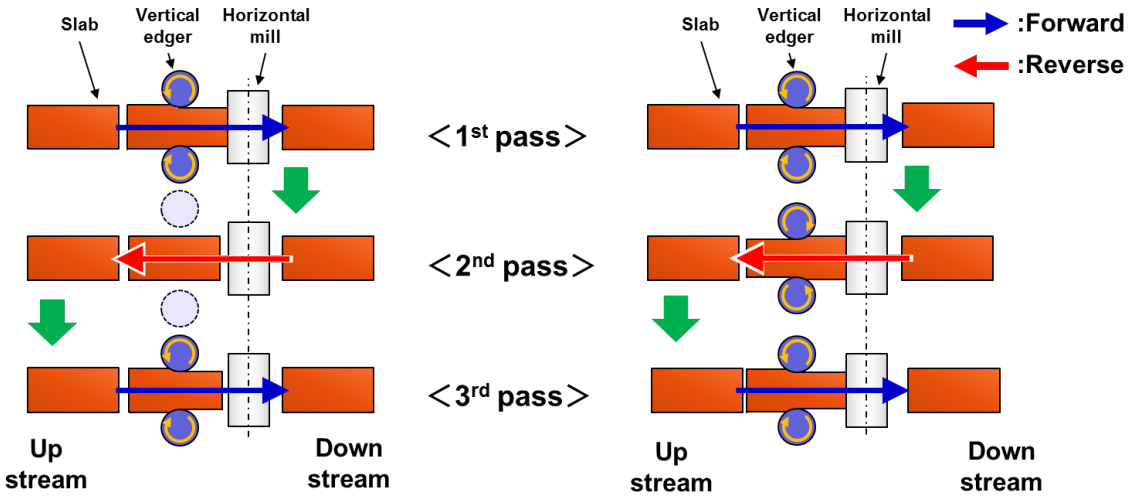

Figure 3: Roughing mill rolling sequence of standard rolling and VVH rolling

3 WIDTH DEFORMATION MECHANISM AT ROUGHING STAND

A considerable number of studies have been constructed on the prediction of width deformation in the roughing mill due to the importance of this process in achieving width accuracy precision. Shibahara et al. [1] had described the width deformation in a roughing mill with standard vertical edger rolling using equation 1:

$$B_x = B_E + \Delta B_D + \Delta B_H \tag{1}$$

where, B_x is delivery width, B_E is width after vertical edger rolling, ΔB_D is width spread due to the reduction of protrusions which appear at both width ends of the slab after vertical edger rolling (the protrusions are often called as "dog-bone" due to the visual appearance of the cross-sectional shape of the slab), and ΔB_H is ordinary width spread caused by horizontal rolling.

In a past, width deformation phenomena using the standard roughing mill sequence had been well studied [2, 3]. However, width deformation phenomena when using the VVH rolling sequence has received little study.

4 ANALYSIS CONDITIONS OF FINITE ELEMENT METHOD

An analysis of VVH rolling was done using finite element methods. The length and thickness of the entry slab were fixed at 4500mm and 200 mm for this analysis. Thickness reduction was 15% of the entry slab thickness. Slab widths and total width draft is shown in Table 1. In this paper, "total width draft" ($\Delta B_{rev} + \Delta B_{fwd}$) is defined as the total width draft achieved using both a forward and a reverse pass. In addition, "reverse pass distribution ratio" (β_{rev}), is calculated using equation 2:

$$\beta_{rev} = \frac{\Delta B_{rev}}{\Delta B_{rev} + \Delta B_{fwd}} \tag{2}$$

Table 1: The conditions of entry slab width, total width draft and reverse pass distribution ratio

Entry slab width [mm]	800, 1400, 2000
Total width draft [mm]	50, 100, 150
Reverse pass distribution ratio [-]	0, 0.1, 0.25, 0.33, 0.5, 0.67, 0.75, 0.9, 1.0

Figure 4 shows the overview of FEM 3-dimensional modeling. Due to the symmetry of thickness and width over the length of the slab, quartered 3-dimensional modeling was utilized in the simulation. To obtain a clear analysis of the effect of total width reduction using two passes, a rectangular slab was fed into vertical edger in the reverse pass direction then turned for a forward pass. During the forward pass, width was reduced using the vertical edger and thickness was reduced using the horizontal with the edger mill and horizontal mill working in tandem.

The work roll diameters of the vertical edger and the horizontal mill were 1200 mm. Both vertical edger rolls and horizontal mill rolls were defined as rigid bodies since roll deformation during rolling is not significant relative to the deformation of the slab. The contact between the surface of the slab and the vertical edger rolls and the contact between the surface of the slab and the horizontal mill rolls were modeled using applied penalty methods.

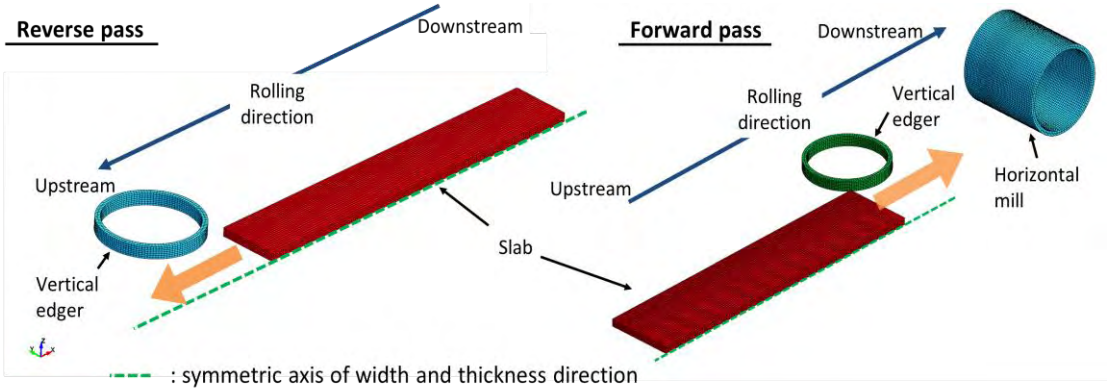

Figure 4: FEM 3-dimensional modeling at a forward pass and at a reverse pass

The mesh size, the number of mesh size, values for the slabs are shown in Table 2. The mesh size and the number of mesh at the edge side of the slab in the width direction, the middle part of the slab in the width direction, and the centerline of the slab, took the values from left to right at the column in 1400mm and 2000mm of the slab width. To simulate detailed behavior at the edge of the slab in the width direction, the mesh size at the edge of the slab was setup to be smaller than at the centerline of the slab.

Table 2: A mesh size and number of mesh for a slab

		Mesh size [mm]	Number of mesh [-]
Entry slab length		30	150
Entry slab thickness		20	5
Entry slab width [mm]	800	25	16
	1400	25, 30, 35	11, 6, 7
	2000	25, 30, 35	14, 10, 10

Material properties of the slab is shown in Table 3. The slab was defined as elastoplastic body. The simulation accuracy might be worse if the stress propagation speed is faster as passing through more than a mesh during a calculation time step. So that, applying properly Young's modulus and density is prefer. However, the stress propagation speed is slower than work speed in this process, so that the value of Young's modulus at room temperature was used. Also, the density was mass-scaled as 1/10. Those allowed to shorten computation time. Strain-hardening exponent and strain rate exponent were defined as the values calculated using Misaka's equation [4].

Table 3: Material properites of the slab

Item	Value	Unit
Density (before mass-scaling)	7850	kg/m^3
Young's modulus	210000	MPa
Poisson's ratio	0.3	-
Deformation resistance (at 1000 ºC)	120	MPa
Strain-hardening exponent	0.21	-
Strain rate exponent	0.13	-
Friction coefficient	0.4	-

5 ANALYSIS RESULTS

The FEM simulation results were evaluated according to three factors:
(1) The amount of width spread when using VVH rolling ($\Delta B_D + \Delta B_H$)
(2) The dog-bone shape
(3) Width fluctuation at head end and tail end when using VVH rolling

5.1 Width spread after roughing mill

The relationship of the reverse pass distribution ratio and the width spread when using VVH rolling is shown in Figure 5. In Figure 5a, the entry slab width is constant at 2000 mm, and the total width draft changed from 50 mm to 150 mm respectively. In Figure 5b, the total width draft is constant at 100 mm, and the entry slab width changed from 800 mm to 2000 mm respectively. Width draft limits are shown as dotted lines in both Figure 5a and Figure 5b.

Regardless of the entry slab width and the total width draft, width spread is reaches the maximum level when the reverse pass distribution ratio equals 0.5 (forward pass width draft equal to reverse pass width draft). This is affected by the highest dog-bone peak height h_d as shown in Figure 6 of section 5.2. Width spread will be reduced when the target width draft for the forward pass does not equal the target width draft for the reverse pass and the condition where they are equal should be avoided. A reverse pass distribution ratio less than 0.5 will result in lower width spread than a reverse pass distribution ratio greater than 0.5. In addition, width spread will increase when entry slab width increases and when total width draft increases.

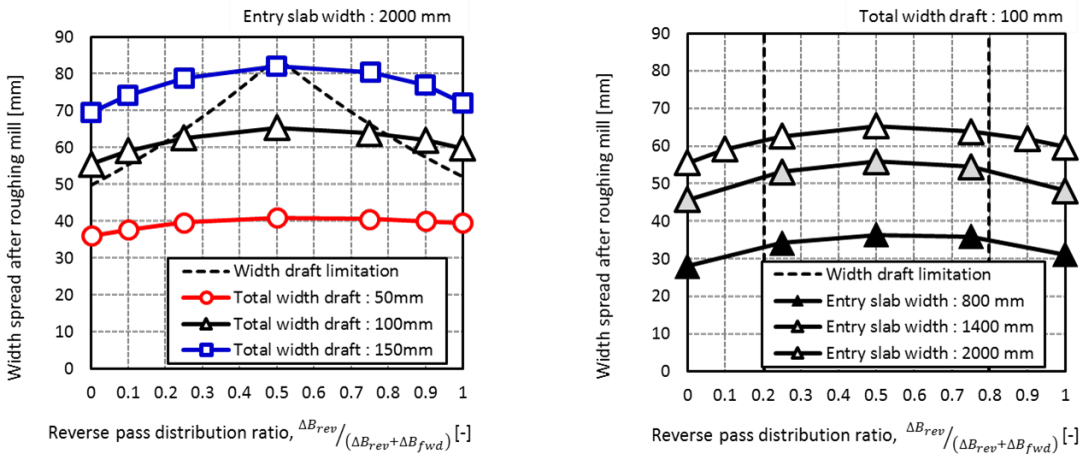

5a **5b**

Figure 5: The relationship of the reverse pass distribution ratio and the width spread using VVH rolling (a: entry slab width constant at 2000 mm, b: total width draft constant at 100 mm)

5.2 Dog-bone shape

The dog-bone shape of the slab effects the width spread when using VVH rolling. To evaluate the relationship of the reverse pass distribution ratio and dog-bone shape after forward pass vertical edger rolling, dog-bone shape is defined using a dog-bone peak height ratio and a dog-bone peak position ratio. These parameters are shown in Figure 6 and calculated using equations 3 and 4:

$$\gamma_{height} = \frac{h_D}{h_C} \tag{3}$$

$$\gamma_{position} = \frac{B_D}{B_C} \tag{4}$$

where, h_D is the dog-bone peak height, h_C is the slab thickness at center line of the slab, B_D is the left edge dog-bone peak position to the right edge dog-bone peak distance (measured across the strip width), B_C is the slab width.

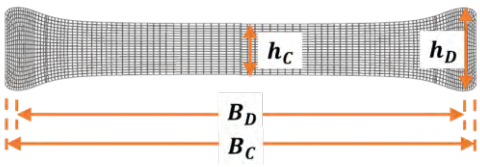

Figure 6: The cross-section shape of dog-bone and definitions of dog-bone peak height raito and dog-bone peak position ratio

The relationship of the reverse pass distribution ratio and the dog-bone peak height ratio is shown in Figure 7. The relationship of the reverse pass distribution ratio and the dog-bone peak position ratio is shown in Figure 8. In Figure7a and 8a, the entry slab width is constant at 2000 mm. The total width draft is constant at 100 mm in Figure 7b and 8b. The dog-bone peak height

ratio is the greatest when the reverse pass distribution ratio equals 0.5. The highest width spread using VVH rolling when the width draft for the forward pass equals the width draft for the reverse pass is affected by the highest dog-bone peak height as shown in Figure 6.When the reverse pass distribution ratio is greater than 0.5, the dog-bone peak height is less than when the reverse pass ratio is less than 0.5. The greatest dog-bone peak position ratio occurs when the reverse pass distribution ratio equals 0.75. This dog-bone peak position tendency affects the width spread when using VVH rolling to a slightly greater degree when the reverse distribution ratio is more than 0.5.

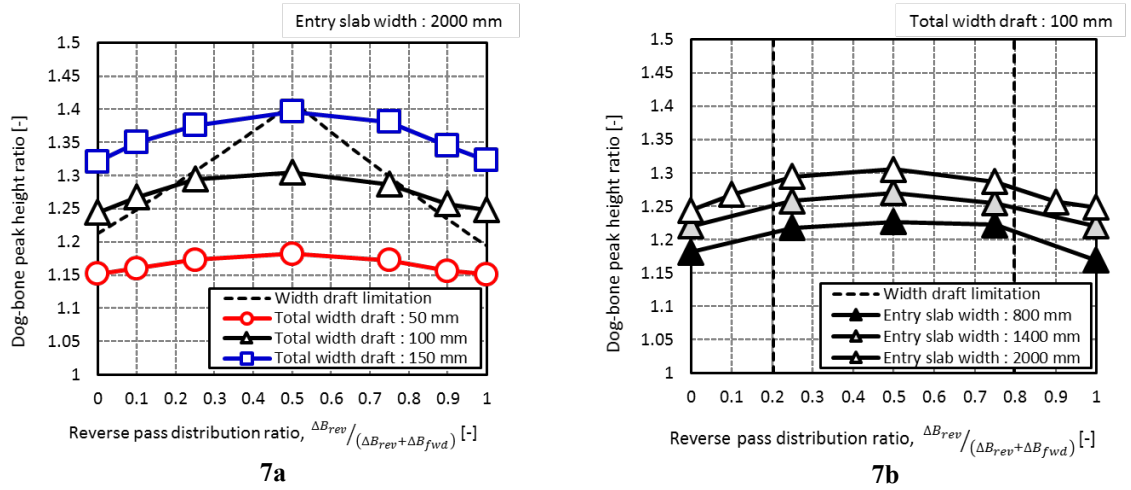

7a **7b**

Figure 7: The relationship of the reverse pass distribution ratio and the dog-bone peak height ratio (a: entry slab width constant at 2000 mm, b: total width draft constant at 100 mm)

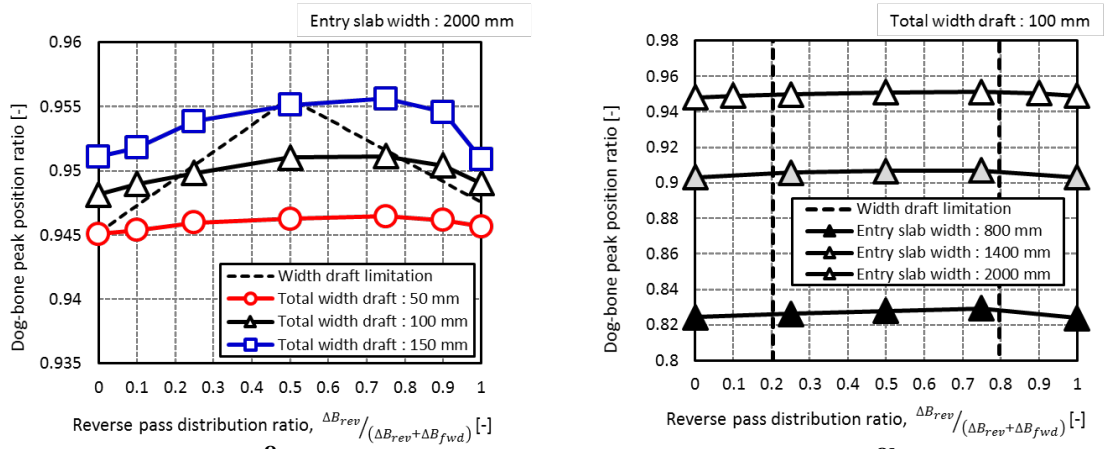

8a **8b**

Figure 8: The relationship of the reverse pass distribution ratio and the dog-bone peak position ratio (a: entry slab width constant at 2000 mm, b: total width draft constant at 100 mm)

5.3 Width at head end and tail end

Unsteady width deformation in head and tail part is also an important factor to consider when evaluating the behavior of VVH rolling. The definitions of width fluctuation at head end and

tail end are shown in Figure 9. The width fluctuations at head and tail end are defined as the amount of width narrowing toward the body portion of the slab. The head end of the slab is the front edge, in the length direction, during forward passes. Figure 10 shows the relationship of the reverse pass distribution ratio and width fluctuation at head and tail end. Figure 10a shows the results for the tail end and Figure 10b shows the results for the head end. For head end, a greater reverse pass distribution ratio results in lower width fluctuation. The highest width fluctuation occurs when the reverse pass distribution ratio is equal to 0.25. For tail end, a greater reverse pass distribution ratio results in higher width fluctuations.

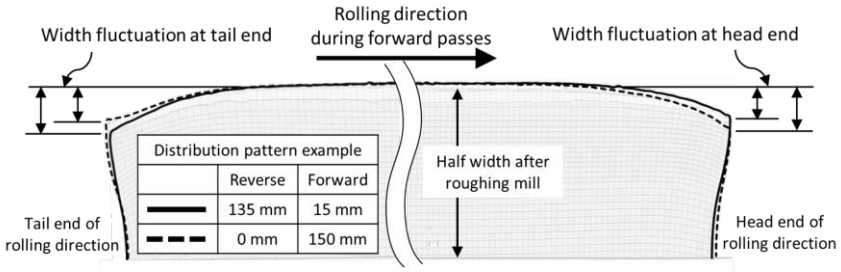

Figure 9: top view of examples when using VVH rolling and definitions of the amount of width fluctuation at head and tail end (deformation 3 times as real)

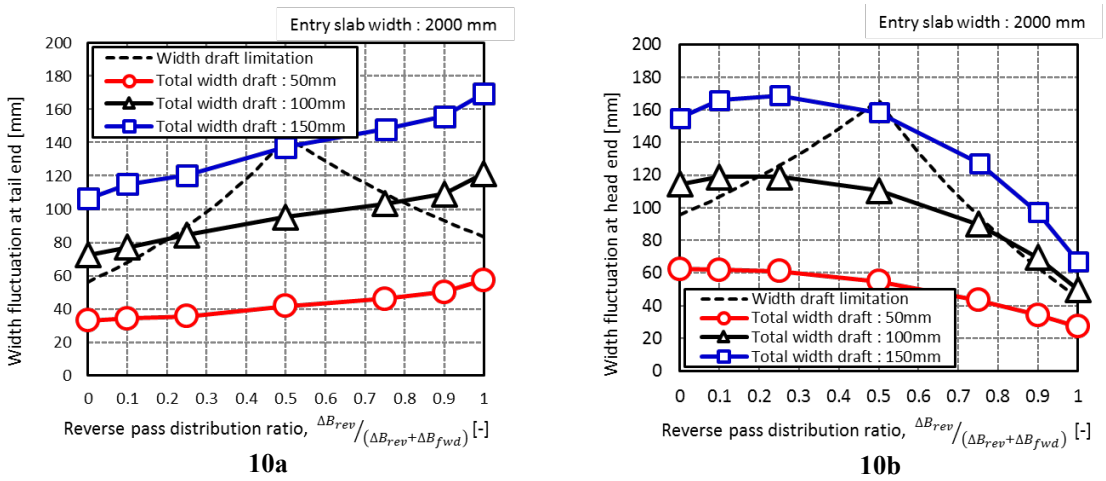

10a **10b**

Figure 10: The relationship of the reverse pass distribution ratio and width fluctuation at head and tail end (a: tail end, b: head end)

The following table summarizes the analysis of the results:

Table 4: Summary of analysis results

	Reverse pass distribution ratio		
	Low	0.5	High
Width spread when VVH rolling	Small	Big	Small
Dog-bone peak height	Low	High	Low
Dog-bone peak position	Close to center		Close to edge
Width fluctuation at head end	Big		Small
Width fluctuation at tail end	Small		Big

5.4 Evaluation of optimal distribution pattern

Analysis results were used to determine the optimal distribution pattern of width draft between a forward pass and a reverse pass using VVH rolling. The conditions for better width shape were determined from the relationship of reverse pass distribution ratio and width spread when using VVH rolling, dog-bone shape, and width fluctuation at head and tail end. We defined scores $K^n_{\beta_{rev}}$ of width spread when using VVH rolling, dog-bone shape, and width fluctuation at head and tail end with equation 5:

$$K^n_{\beta_{rev}} = \omega_n \cdot \left(\delta^n_{\beta_{rev}} - \delta^n_{\beta_{rev\_min}}\right) \tag{5}$$

Where, β_{rev} is the reverse pass distribution ratio, n is each width feature such as width spread when using VVH rolling, dog-bone shape, and width fluctuation at head and tail end, ω_n is weight parameter for each feature, $\delta^n_{\beta_{rev}}$ is feature value at each reverse pass distribution ratio, $\delta^n_{\beta_{rev\_min}}$ is the worst value of the feature. A weight parameter for a feature takes the score to be "0" as the worst value in a feature, and to be "0.2" as the best value in a feature.

The relationship of the reverse pass distribution ratio and each score in total width draft 100 mm are shown in Figure 11. The scores can evaluate as below:

- Higher width draft on a forward pass leads to lower width spread and this increases width reduction efficiency.
- Higher width draft on a reverse pass decreases dog-bone peak height ratio. However, this increases dog-bone peak position ratio.
- Higher width draft on a forward pass decreases width fluctuation at the head end. Higher width draft on a reverse pass lowers width fluctuation at the tail end.

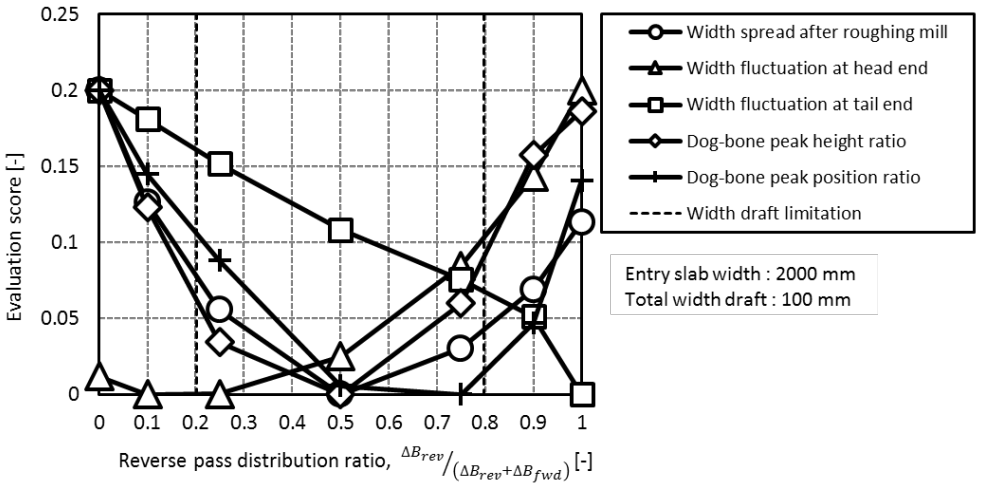

Figure 11: The relationship of reverse pass distribution ratio and evalucation score for each feature (Entry slab width: 2000mm, total width draft: 100mm)

Furthermore, sum of the scores can be used to determine the optimal distribution pattern between a forward pass and a reverse pass based on the combined effect on all the important width measurements. The total score for each reverse pass distribution ratio for entry slab width equals 2000mm is shown in Figure 12. As concern of the width draft limits, the reverse pass

distribution ratio around 0.25 can be identified as the optimal distribution pattern for total width draft equal to 100mm.

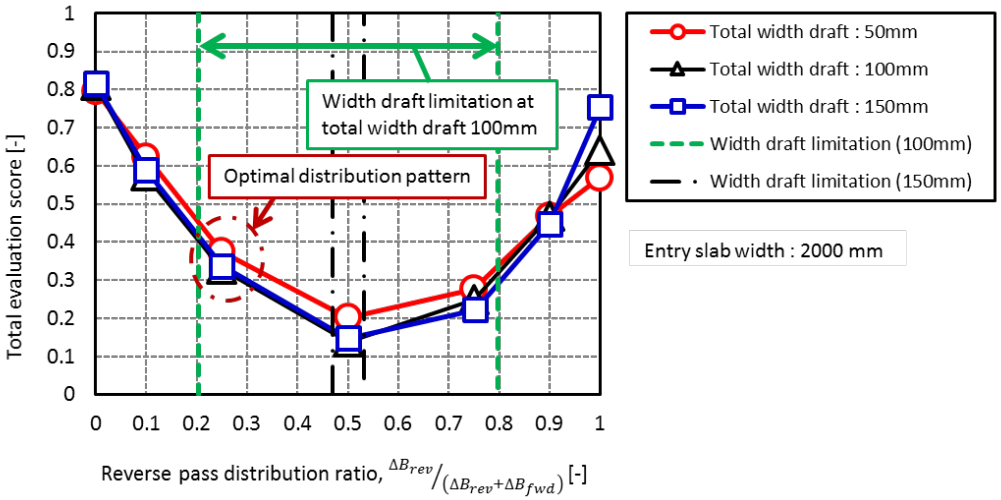

Figure 12: The relationship of reverse pass distribution ratio and total evaluation score (Entry slab width: 2000mm)

6 CONCLUSIONS

The width reduction process in roughing mill stand in a hot strip mill which reduces slab width using both forward and reverse passes was simulated using 3-dimensional FEM. The influence of various conditions and their deformation phenomena were studied. The results allowed the following conclusions:

- The characteristic of width deformation using VVH rolling including width spread, dog-bone peak height and peak position, and width fluctuation at head and tail ends of the slab were analyzed and summarized in Table 4.
- A little higher width draft during forward passes than during reverse passes can be proposed as the optimal distribution pattern based on the evaluation scores.
- FEM analysis concerned with the temperature drop from a pass to next pass will be future work.

REFERENCES

[1] T.Shibahara, R.Takahashi, T.Nunokawa, S.Kubota, “Automatic Width Control System at Roughing Train in Hot Strip Mill”, Advanced Technology of Plasticity, vol. II, 1200-1205, (1986). (in Japanese)

[2] S.Osada, F.Kamiyama, M.Kawaharada, H.Nakajima, S.Yanagimoto, Proceedings of the Japanese Spring Conference for the Technology of Plasticity, 125-128, (1977). (in Japanese)

[3] S.Hamauzu, H.Tokita, K.Ishii, M.Kawaharada, “Experiments by Using Lead on the Control Method of Width Drop at the Top and Tail Ends of Hot Strip”, Journal of the Japan Society for Technology of Plasticity, vol. 25, No. 277, 143-152, (1984). (in Japanese)

[4] Y.Misaka, T.Yoshimoto, Journal of the Japan Society for Technology of Plasticity, 8, 414, (1967). (in Japanese)